Article

Unprecedented Head-to-Head Conformers of d(GpG) Bound to the Antitumor Active Compound Tetrakis (□-carboxylato)dirhodium(II,II)

Helen T. Chifotides, Karl M. Koshlap, Lisa M. Prez, and Kim R. Dunbar

J. Am. Chem. Soc., **2003**, 125 (35), 10703-10713• DOI: 10.1021/ja027779s • Publication Date (Web): 09 August 2003

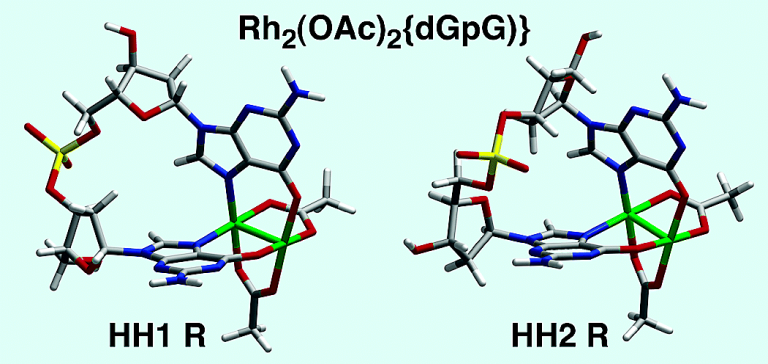

More About This Article

Additional resources and features associated with this article are available within the HTML version:

- Supporting Information
- Links to the 7 articles that cite this article, as of the time of this article download
- Access to high resolution figures
- Links to articles and content related to this article
- Copyright permission to reproduce figures and/or text from this article

View the Full Text HTML

Journal of the American Chemical Society is published by the American Chemical Society. 1155 Sixteenth Street N.W., Washington, DC 20036

J|A|C|S
ARTICLES
Published on Web 08/09/2003

Unprecedented Head-to-Head Conformers of d(GpG) Bound to the Antitumor Active Compound Tetrakis (μ-carboxylato)dirhodium(II,II)

Helen T. Chifotides,*,† Karl M. Koshlap,‡ Lisa M. Pérez,§ and Kim R. Dunbar*,†

Contribution from the Department of Chemistry and the Department of Biochemistry and Biophysics, Texas A&M University, College Station, Texas 77843

Received July 19, 2002; E-mail: chifotides@mail.chem.tamu.edu; dunbar@mail.chem.tamu.edu

Abstract: The *N7/O6 equatorial* binding interactions of the antitumor active complex $Rh_2(OAc)_4(H_2O)_2$ ($OAc^- = CH_3CO_2^-$) with the DNA fragment d(GpG) have been unambiguously determined by NMR spectroscopy. Previous X-ray crystallographic determinations of the *head-to-head* (HH) and *head-to-tail* (HT) adducts of dirhodium tetraacetate with 9-ethylguanine (9-EtGH) revealed *unprecedented* bridging *N7/O6* guanine nucleobases that span the Rh−Rh bond. The absence of *N7* protonation at low pH and the notable *increase* in the acidity of *N1−H* ($pK_a \approx 5.7$ as compared to 8.5 for *N7 only* bound platinum adducts), suggested by the pH dependence titrations of the purine H8 ^{1}H NMR resonances for $Rh_2(OAc)_2(9\text{-}EtG)_2$ and $Rh_2(OAc)_2$-{d(GpG)}, are consistent with bidentate *N7/O6* binding of the guanine nucleobases. The pK_a values estimated for *N1−H* (de)protonation, from the pH dependence studies of the C6 and C2 ^{13}C NMR resonances for the $Rh_2(OAc)_2(9\text{-}EtG)_2$ isomers, concur with those derived from the H8 ^{1}H NMR resonance titrations. Comparison of the ^{13}C NMR resonances of C6 and C2 for the dirhodium adducts $Rh_2(OAc)_2(9\text{-}EtG)_2$ and $Rh_2(OAc)_2${d(GpG)} with the corresponding resonances of the unbound ligands {at pH 7.0 for 9-EtGH and pH 8.0 for d(GpG)}, shows substantial *downfield* shifts of $\Delta\delta \approx 11.0$ and 6.0 ppm for C6 and C2, respectively; the latter shifts reflect the effect of *O6* binding to the dirhodium centers and the ensuing enhancement in the acidity of *N1−H*. Intense H8/H8 ROE cross-peaks in the 2D ROESY NMR spectrum of $Rh_2(OAc)_2${d(GpG)} indicate *head-to-head* arrangement of the guanine bases. The $Rh_2(OAc)_2${d(GpG)} adduct exhibits two major *right-handed* conformers, HH1 R and HH2 R, with HH1 R being three times more abundant than the unusual HH2 R. Complete characterization of both adducts revealed repuckering of the 5′-G sugar rings to C3′-endo (N-type), retention of C2′-endo (S-type) conformation for the 3′-G sugar rings, and *anti* orientation with respect to the glycosyl bonds. The structural features obtained for $Rh_2(OAc)_2${d(GpG)} by means of NMR spectroscopy are very similar to those for *cis*-[$Pt(NH_3)_2${d(GpG)}] and corroborate molecular modeling studies.

Introduction

Cisplatin {*cis*-$[Pt(NH_3)_2Cl_2]$ *cis*-DDP} is one of the most widely used drugs in the treatment of cancer.[1] Extensive investigations of this potent antitumor agent have established DNA as its primary intracellular target. In particular, the most abundant *cis*-DDP DNA adduct has been determined to be a *head-to-head* (HH) 1,2-intrastrand cross-link between adjacent guanine nucleobases {d(GpG)}; the latter sites account for 65% of the bound platinum and are the primary inhibitors of transcription and DNA replication.[1,2] Structural details of the platinated d(GpG) adducts, obtained from single-crystal X-ray diffraction studies,[3] have been complemented by high-resolution NMR spectroscopy[4] combined with molecular modeling.[5] The platinated HH cross-links, which cause the DNA duplex to bend and unwind,[6a] are uniquely recognized by cellular

* Authors to whom correspondence should be addressed.
† Department of Chemistry, Texas A&M University.
‡ Department of Biochemistry and Biophysics, Texas A&M University.
§ Laboratory for Molecular Simulation, Texas A&M University.

(1) (a) Lippard, S. J. *Pure and Appl. Chem.* **1987**, *59*, 731−742. (b) Bloemink, M. J.; Reedijk, J. In *Metal Ions in Biological Systems*; Sigel, A., Sigel, H., Eds.; Marcel Dekker: New York, 1996; Vol. 32, pp 641−685. (c) Reedijk, J. *Chem Commun.* **1996**, 801−806. (d) *Cisplatin: Chemistry and Biochemistry of a Leading Anticancer Drug*; Lippert, B., Ed.; Wiley-VCH: Weinheim, 1999; pp 1−556. (e) Jamieson, E. R.; Lippard, S. J. *Chem. Rev.* **1999**, *99*, 2467−2498. (f) Cohen, S. M.; Lippard, S. J. *Prog. Nucl. Acid Res. Mol. Biol.* **2001**, *67*, 93−130. (g) Hambley, T. W. *J. Chem. Soc., Dalton Trans.* **2001**, 2711−2718.

(2) (a) Zlatanova, J.; Yaneva, J.; Leuba, S. H. *FASEB J.* **1998**, *12*, 791. (b) Zhai, X.; Beckmann, H.; Jantzen, H.-M.; Essigmann, J. M. *Biochemistry*, **1998**, *37*, 16307.

(3) (a) Sherman, S. E.; Gibson, D.; Wang, A. H.-J. and Lippard, S. J. *Science*, **1985**, *230*, 412. (b) Admiraal, G.; van der Veer, J. L.; de Graaff, R. A. G.; den Hartog, J. H. J.; Reedijk, J. *J. Am. Chem. Soc.* **1987**, *109*, 592. (c) Sherman, S. E.; Gibson, D.; Wang, A. H.-J. and Lippard, S. J. *J. Am. Chem. Soc.* **1988**, *110*, 7368. (d) Takahara, P. M.; Rosenzweig, A. C.; Frederick, C. A.; Lippard, S. J. *Nature* **1995**, *377*, 649. (e) Takahara, P. M.; Frederick, C. A.; Lippard, S. *J. Am. Chem. Soc.* **1996**, *118*, 12309.

(4) (a) Girault, J. P.; Chottard, G.; Lallemand, J.-Y. and Chottard, J.-C. *Biochemistry*, **1982**, *21*, 1352. (b) den Hartog, J. H. J.; Altona, C.; Chottard, J. C.; Girault, J. P.; Lallemand, J.-Y.; de Leeuw, F. A. A. M.; Marcelis, A. T. M. and Reedijk, J. *Nucleic Acids Res.* **1982**, *10*, 4715. (c) den Hartog, J. H. J.; Altona, C.; van Boom, J. H.; van der Marel, G. A.; Haasnoot, C. A. G. and Reedijk, J. *J. Am. Chem. Soc.* **1984**, *106*, 1528. (d) den Hartog, J. H. J.; Altona, C.; van Boom, J. H.; van der Marel, G. A.; Haasnoot, C. A. G.; Reedijk, J. *J. Biomol. Struct. Dyn.* **1985**, *2*, 1137. (e) Iwamoto, M.; Mukundan, S. Jr.; Marzilli, L. G. *J. Am. Chem. Soc.* **1994**, *116*, 6238. (f) Yang, D.; van Boom S. S. G. E.; Reedijk, J.; van Boom, J. H.; Wang, A. H. J. *Biochemistry* **1995**, *34*, 12912. (g) Gelasko, A.; Lippard, S. J. *Biochemistry*, **1998**, *37*, 9230.

Chart 1. Structure and Atom Numbering of (a) Nucleobase 9-Ethylguanine (9-EtGH) and (b) Dinucleotide d(GpG)

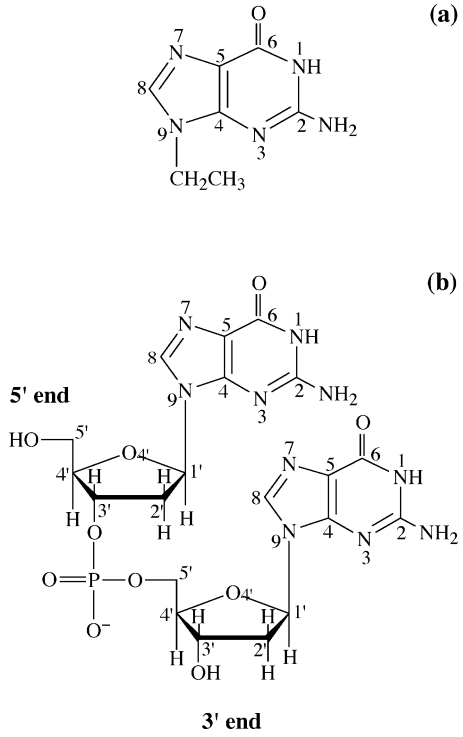

proteins containing the high-mobility group (HMG) domains involved in vital cellular repair processes.[2,6b−d]

In light of the importance of platinum-DNA interactions and the relative ease of characterization of nucleobase complexes, the latter have been used to model longer DNA adducts. For the vast majority of *cis*-DDP adducts with untethered purines (Chart 1a), the *head-to-tail* (HT) isomers are preferred.[7−11] Conversely, for platinum adducts with tethered guanine bases, *i.e.*, guanine units linked by phosphodiester bonds (Chart 1b), the HH conformers exclusively dominate.[3,4,12−14] This strong preference is attributed to the restrictions imposed by the sugar−phosphate backbone linking the adjacent guanine bases, as well as to GC Watson−Crick base pairing.[15] It has recently been shown, however, that in systems where the rapid dynamic motion of the d(GpG) adduct is restricted by chiral, bulky, tethered ligands bound to the platinum, HT conformers of the adducts are stabilized.[16,17]

Chart 2. Structure of Metal−Metal Bonded Dirhodium Compounds with Carboxylate Ligands

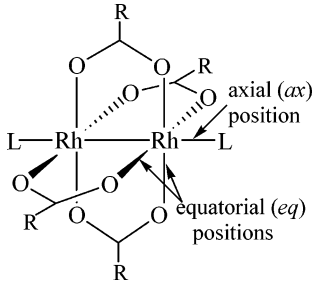

Recently, work in our laboratories has unearthed unusual DNA binding modes for an entirely different class of antitumor transition metal compounds whose structure and ligand environment are quite different from those of *cis*-DDP. Specifically, these are dinuclear metal−metal bonded dirhodium compounds $Rh_2(O_2CR)_4L_2$ (R = Me, Et, Pr; L = solvent) that contain at least two bridging carboxylate ligands (Chart 2).[18] It has been noted that, in a manner akin to the *cis*-DDP anticancer reactivity, dirhodium compounds also inhibit DNA replication and protein synthesis.[19] A perusal of the literature reveals that dirhodium compounds exhibit preferential binding to adenine as compared to guanine.[19a,b,20] The reactivity of guanine is much slower due to steric repulsions between the ketone *O6* and the carboxylate oxygen atoms.[20e,h] Recently, we unequivocally established that $Rh_2(OAc)_4$ eventually forms thermodynamically stable substitution products that involve *unprecedented* equato-

(5) (a) Kozelka, J.; Archer, S.; Petsko, G. A.; Lippard, S. J. and Quigley, G. J. *Biopolymers* **1987**, *26*, 1245. (b) Kozelka, J.; Chottard, J.-C. *Biophys. Chem.* **1990**, *35*, 165. (c) Kozelka, J.; Fouchet, M.-H.; Chottard, J.-C. *Eur. J. Biochem.* **1992**, *205*, 895. (d) Lemaire, D.; Fouchet, M.-H.; Kozelka, J. *J. Inorg. Biochem.* **1994**, *53*, 261−271. (e) Yao, S.; Plastaras, J. P. and Marzilli, L. G. *Inorg. Chem.* **1994**, *33*, 6061. (f) Kozelka, J. In *Metal Ions in Biological Systems*; Sigel, A., Sigel, H., Eds.; Marcel Dekker: New York, 1996; Vol. 33, pp 1−28. (g) Hambley, T. W.; Jones, A. R. *Coord. Chem. Rev.* **2001**, *212*, 35.

(6) (a) Rice, J. A.; Crothers, D. M.; Pinto, A. L.; Lippard, S. J. *Proc. Natl. Acad. Sci. U.S.A.* **1988**, *85*, 4158. (b) Huang, J.-C.; Zamble, D. B.; Reardon, J. T.; Lippard, S. J.; Sancar, A. *Proc. Natl. Acad. Sci. U.S.A.* **1994**, *91*, 10 394. (c) Zamble, D. B.; Mu, D.; Reardon, J. T.; Sancar, A.; Lippard, S. J. *Biochemistry* **1996**, *35*, 10004. (d) Ohndorf, U.-M.; Rould, M. A.; He, Q.; Pabo, C. O.; Lippard, S. J. *Nature* **1999**, *399*, 708.

(7) Lippert, B. *Prog. Inorg. Chem.* **1989**, *37*, 1.

(8) Marzilli, L. G.; Marzilli, P. A.; Alessio, E. *Pure Appl. Chem.* **1998**, *70*, 961.

(9) (a) Lippert, B.; Raudaschl, G.; Lock, C. J. L.; Pilon, P. *Inorg. Chim. Acta*, **1984**, *93*, 43. (b) Schöllhorn, H.; Raudaschl-Sieber, G.; Müller, G.; Thewalt, U.; Lippert, B. *J. Am. Chem. Soc.* **1985**, *107*, 5932. (c) Schröder, G.; Kozelka, J.; Sabat, M.; Fouchet, M.-H.; Beyerle-Pfnür, R.; Lippert, B. *Inorg. Chem.* **1996**, *35*, 1647. (d) Schröder, G.; Sabat, M.; Baxter, I.; Kozelka, J.; Lippert, B. *Inorg. Chem.* **1997**, *36*, 490.

(10) Marzilli, L. G.; Iwamoto, M.; Alessio, E.; Hansen, L. and Calligaris, M. *J. Am. Chem. Soc.* **1994**, *116*, 815.

(11) Kiser, D.; Intini, F. P.; Xu, Y.; Natile, G. and Marzilli, L. G. *Inorg. Chem.* **1994**, *33*, 4149.

(12) Berners-Price, S. J.; Ranford, J. D.; Sadler, P. J. *Inorg. Chem.* **1994**, *33*, 5842.

(13) (a) Qu, Y.; Bloemink, M. J.; Reedijk, J.; Hambley, T. W.; Farrell, N. *J. Am. Chem. Soc.* **1996**, *118*, 9307. (b) Hambley, T. W.; Ling, E. C. H.; Messerle, B. A. *Inorg. Chem.* **1996**, *35*, 4663.

(14) Ano, S. O.; Kuklenyik, Z.; Marzilli, L. G. In *Cisplatin: Chemistry and Biochemistry of a Leading Anticancer Drug*; Lippert, B., Ed.; Wiley-VCH: Weinheim, 1999; pp 247−291.

(15) Marzilli, L. G.; Intini, F. P.; Kiser D.; Wong, H. C.; Ano, S. O.; Marzilli, P. A.; Natile, G. *Inorg. Chem.* **1998**, *37*, 6898.

(16) (a) Ano, S. O.; Intini, F. P.; Natile, G.; Marzilli, L. G. *J. Am. Chem. Soc.* **1998**, *120*, 12 017. (b) Marzilli, L. G.; Ano, S. O.; Intini, F. P.; Natile, G. *J. Am. Chem. Soc.* **1999**, *121*, 9133, and references therein. (c) Williams, K. M.; Cerasino, L.; Natile, G.; Marzilli, L. G. *J. Am. Chem. Soc.* **2000**, *122*, 8021. (d) Sullivan, S. T.; Ciccarese, A.; Fanizzi, F. P.; Marzilli, L. G. *J. Am. Chem. Soc.* **2001**, *123*, 9345, and references therein.

(17) Sullivan, S. T.; Saad, J. S.; Fanizzi, F. P.; Marzilli, L. G. *J. Am. Chem. Soc.* **2002**, *124*, 1558.

(18) Cotton, F. A.; Walton, R. A. Multiple Bonds Between Metal Atoms; Clarendon Press: Oxford, 1993; Chapter 7, pp 431−501.

(19) (a) Erck, A.; Rainen, L.; Whileyman, J.; Chang, I.; Kimball, A. P.; Bear, J. L. *Proc. Soc. Exp. Biol. Med.* **1974**, *145*, 1278. (b) Bear, J. L.; Gray, H. B.; Rainen, L.; Chang, I. M.; Howard, R.; Serio, G.; Kimball, A. P. *Cancer Chemother. Rep.* Part I **1975**, *59*, 611. (c) Howard, R. A.; Spring, T. G.; Bear, J. L. *Cancer Res.* **1976**, *36*, 4402. (d) Erck, A.; Sherwood, E.; Bear, J. L.; Kimball, A. P. *Cancer Res.* **1976**, *36*, 2204. (e) Howard, R. A.; Sherwood, E.; Erck, A.; Kimball, A. P.; Bear, J. L. *J. Med. Chem.* **1977**, *20*, 943. (f) Howard, R. A.; Kimball, A. P. Bear, J. L. *Cancer Res.* **1979**, *39*, 2568. (g) Rao, P. N.; Smith, M. L.; Pathak, S.; Howard, R. A.; Bear, J. L. *J. Nat. Cancer Inst.* **1980**, *64*, 905. (h) Hall, L. M.; Speer, R. J.; Ridgway, H. J. *J. Clin. Hematol. Oncol.* **1980**, *10*, 25. (i) Bear, J. L. In *Precious Metals 1985: Proceedings of the Ninth International Precious Metals Conference*; Zysk, E. D.; Bonucci, J. A., Eds.; Int. Precious Metals: Allentown, PA, 1986; pp 337−344.

(20) (a) Rainen, L.; Howard, R. A.; Kimball, A. P.; Bear, J. L. *Inorg. Chem.* **1975**, *14*, 2752. (b) Pneumatikakis, G.; Hadjiliadis, N. *J. Chem. Soc., Dalton Trans.* **1979**, 596. (c) Farrell, N. *J. Chem. Soc., Chem. Commun.* **1980**, 1014. (d) Aoki, K.; Yamazaki, H. *J. Chem. Soc., Chem. Commun.*, **1980**, 186. (e) Farrell, N. *J. Inorg. Biochem.* **1981**, *14*, 261. (f) Rubin, J. R. Sundaralingam, M. *J. Biomol. Struct. Dyn.* **1984**, *2*, 525. (g) Alberding, N.; Farrell, N.; Crozier, E. D. *J. Am. Chem. Soc.* **1985**, *107*, 384. (h) Rubin, J. R.; Haromy, T. P.; Sundaralingam, M. *Acta Crystallogr.* **1991**, *C47*, 1712. (i) Aoki, K.; Salam, M. A. *Inorg. Chim. Acta* **2002**, *339*, 427.

Chart 3. (a) *Head-to-Head* (HH) and (b) *Head-to-Tail* (HT) Isomers of $Rh_2(OAc)_2(9\text{-}EtG)_2$

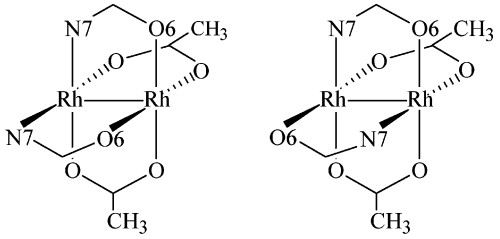

(a) Head-to-Head (HH) (b) Head-to-Tail (HT)

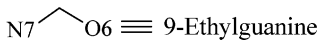

rial *(eq)* bridging interactions with both purines (Chart 3).[21,22] Specifically, in the case of 9-ethylguanine (9-EtGH) (Chart 1a), single-crystal X-ray crystallographic determinations have revealed these bridging modes to involve two 9-EtGH groups spanning the dirhodium unit via the *N7/O6* guanine sites in a *cis* disposition and in a HH or HT orientation (Chart 3).[22] For dirhodium bis-acetate adducts with bridging ligands possessing different types of donor atoms, *e.g.*, 9-EtGH, the compound is designated as HH or HT according to whether the identical atoms of the two ligands are bound to the same or to opposite metal atoms, respectively.[23] It is important to point out that this usage conveniently coincides with the terms HH and HT as used to describe the stacking orientation of purine bases in DNA.

Although *N7*/*O6* bridging of 9-EtGH is unique to metal−metal bonded compounds, there is precedent for purine binding to a metal unit via the ketone *O6*.[24] An important feature of the $Rh_2(OAc)_2(9\text{-}EtG)_2$ adduct is that the purine is deprotonated at *N1*,[22a] *i.e.*, the enolate form of guanine ($9\text{-}EtG^-$) is stabilized (Chart 4b). The importance of the *O6/N1* guanine sites is obvious given that they are involved in Watson−Crick hydrogen bonding in duplex DNA;[25a] alteration of these sites may lead to DNA base mispairing which bears directly on metal mutagenicity and cell death.[25b,c]

The unprecedented *eq* bridging interactions via sites *N7/O6* of the 9-EtGH base spanning the dirhodium unit, in addition to the recent evidence that dirhodium bis-acetate units bind to single-stranded DNA dodecamers that contain GG sites,[26] prompted us to investigate the reactions of $Rh_2(OAc)_4$ with the dinucleotide d(GpG) (Chart 1b), and to compare the structural features of the adduct to those of *cis*-DDP. The structural

Chart 4. (a) Ketone and (b) Enolate Forms of 9-Ethylguanine Bound to the Dirhodium Unit[a]

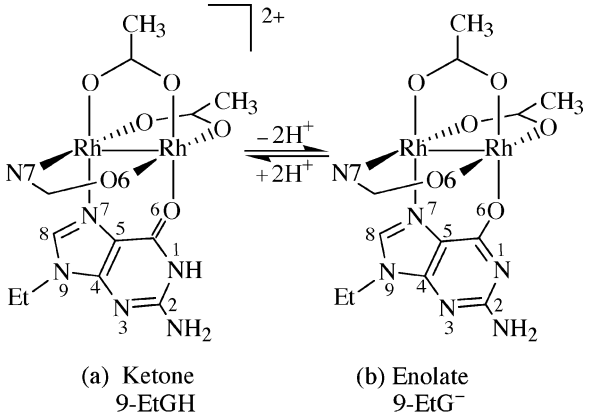

(a) Ketone 9-EtGH (b) Enolate $9\text{-}EtG^-$

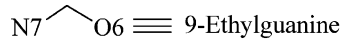

[a] Bond distances are not to scale and angles between atoms are distorted to show structure clearly.

characterization of $Rh_2(OAc)_2\{d(pGpG)\}$ and its remarkable similarities to the crystal structure of *cis*-$[Pt(NH_3)_2\{d(pGpG)\}]$ are discussed in detail in the following article of this issue.[27] Adducts of d(GpG) with dinuclear platinum complexes have been studied, due to the latter being highly active against tumor cell lines resistant to *cis*-DDP.[13a] It is interesting to note that the adduct of the octahedral antitumor complex *trans*-$RuCl_2(DMSO)_4$ with d(GpG) revealed structural features surprisingly similar to those of the corresponding *cis*-DDP adduct.[28] Herein, we report the structural characterization of the $Rh_2(OAc)_2\{d(GpG)\}$ adduct by one- (1D) and two-dimensional (2D) NMR spectroscopy coupled with molecular modeling studies.

Experimental Section

Materials. The reagent 9-ethylguanine (9-EtGH) was purchased from Sigma. The dinucleotide d(GpG) was purchased as the crude DMT (5′-O-dimethoxytrityl) protected material from the Gene Technologies Laboratory at Texas A&M University and purified by reverse phase HPLC; it was used as the sodium salt. Concentrations of the dinucleotide were determined by UV spectroscopy (Shimadzu UV 1601PC spectrophotometer) at 252 nm ($\epsilon_{252} = 2.5 \times 10^4\ M^{-1}cm^{-1}$). Deuterium oxide ($D_2O$, 99.996%), deuterium chloride (DCl, 99.5%), sodium deuteroxide (NaOD, 99.5%) and DSS (Sodium 2,2-Dimethyl-2-Silapentane-5-Sulfonate) were purchased from Cambridge Isotope Laboratories. TMP $\{(CH_3O)_3PO\}$ was purchased from Aldrich.

Syntheses. $Rh_2(OAc)_2(9\text{-}EtG)_2$. The compound was prepared as previously reported.[22a] In a typical reaction, a slurry of 9-EtGH (75 mg, 0.42 mmol) in H_2O (10 mL) was added to a solution of $Rh_2(OAc)_4(H_2O)_2$ (100 mg, 0.21 mmol) in 20 mL of H_2O. The reaction solution was heated at ∼50 °C for approximately 4−5 days, during which time the color gradually changed from aqua to emerald green. Small lyophilized aliquots of the solution were monitored by ^1H NMR spectroscopy to determine the progress of the reaction, and the heating was stopped after no unbound 9-EtGH could be detected (monitored by its H8 proton).

$Rh_2(OAc)_2\{d(GpG)\}$. In a typical reaction, $Rh_2(OAc)_4(H_2O)_2$ (2.5 μmol) in 1 mL of D_2O was treated with d(GpG) (2.5 μmol) in 50 μL

(21) (a) Catalan, K. V.; Mindiola, D. J.; Ward, D. L.; Dunbar, K. R. *Inorg. Chem.* **1997**, *36*, 2458.
(22) (a) Dunbar, K. R.; Matonic, J. H.; Saharan, V. P.; Crawford, C. A.; Christou, G. *J. Am. Chem. Soc.* **1994**, *116*, 2201. (b) Crawford, C. A.; Day. E. F.; Saharan, V. P.; Folting, K.; Huffman, J. C.; Dunbar, K. R. and Christou, G. *Chem. Commun.* **1996**, 1113. (c) Catalan, K. V.; Hess, J. S.; Maloney, M. M.; Mindiola, D. J.; Ward, D. L.; Dunbar, K. R. *Inorg. Chem.* **1999**, *38*, 3904.
(23) Chakravarty, A. R.; Cotton, F. A.; Tocher, D. A. *Inorg. Chem.* **1985**, *24*, 172.
(24) (a) Szalda, D. J.; Kistenmacher, T. J.; Marzilli, L. G. *J. Am. Chem. Soc.* **1976**, *98*, 8371. (b) Gellert, R. W.; Fischer, B. E.; Bau, R. *J. Am. Chem. Soc.* **1980**, *102*, 7812. (c) Cozak, D.; Mardhy, A.; Olivier, M. J.; Beauchamp, A. L. *Inorg. Chem.* **1986**, *25*, 2600. (d) Lorberth, J.; Massa, W.; Essawi, M.-E.; Labib, L. *Angew. Chem., Int. Ed. Engl.* **1988**, *27*, 1160.
(25) (a) Saenger, W. In *Principles of Nucleic Acid Structure*; Cantor, C. R., Ed.; Springer-Verlag: New York, 1984; pp 1−158. (b) Rosenberg, B. *Biochimie* **1978**, *60*, 859. (c) Lippert, B. *J. Am. Chem. Soc.* **1981**, *103*, 5691.
(26) (a) Asara, J. M.; Hess, J. S.; Lozada, E.; Dunbar, K. R.; Allison, J. *J. Am. Chem. Soc.* **2000**, *122*, 8. (b) Chifotides, H. T.; Koomen, J. M.; Kong, M.; Tichy, S. E.; Dunbar, K. R.; Russell, D. H., manuscript in preparation.
(27) Chifotides, H. T.; Koshlap K. M.; Pérez, L. M.; Dunbar, K. R. *J. Am. Chem. Soc.* **2003**, 125, 10714.
(28) Esposito, G.; Cauci, S.; Fogolari, F.; Alessio, E.; Scocchi, M.; Quadrifoglio, F.; Viglino, P. *Biochemistry*, **1992**, *31*, 7094.

of D_2O. The pH of the solution after mixing was 6.0. The sample was incubated at 37 °C for several days, and the progress of the reaction was monitored by ^1H NMR spectroscopy until no unbound d(GpG) could be detected. By the end of the reaction (~12 days), the pH had dropped to 4.7 (the reaction is complete in ~10 days if two molar equivalents of dirhodium complex are used). A distinct emerald green color for the product is observed at pH > 7 (the solubility of the adduct decreases considerably at pH < 6.5). Samples were copiously lyophilized from 99.9% D_2O to remove the acetic acid released during the course of the reaction, and redissolved in 250 μL of 99.996% D_2O for all NMR experiments. MALDI parent ion peak observed at *m*/*z* 917 (Figure S3, Supporting Information).

Instrumentation. The 1D ^1H NMR spectra were recorded on a 500 MHz Varian Inova spectrometer with a 5 mm switchable probehead. The ^1H NMR spectra were typically recorded with 5000 Hz sweep width and 32K data points. A presaturation pulse to suppress the water peak was used when necessary. The 1D ^{13}C NMR spectra were recorded on a 500 MHz Varian Inova spectrometer operating at 125.76 MHz for ^{13}C, and the 1D ^{31}P NMR spectra were recorded on a Varian 300 MHz spectrometer operating at 121.43 MHz for ^{31}P. The ^1H NMR spectra were referenced directly to DSS (Sodium 2,2-Dimethyl-2-Silapentane-5-Sulfonate), whereas the ^{13}C NMR spectra were referenced indirectly to DSS.[29] Trimethyl phosphate (TMP) (0 ppm) was used as an external reference for the ^{31}P NMR spectra. The 1D NMR data were processed using the Varian VNMR 6.1b software.

The 2D NMR data were collected at 5 °C on a Varian Inova 500 MHz spectrometer equipped with a triple-axis gradient penta probe. In general, the homonuclear experiments were performed with a spectral width of ~5000 Hz in both dimensions, whereas some high resolution 2D [$^1H-^1H$] DQF-COSY spectra were collected with 3000 Hz spectral width. 2D [$^1H-^1H$] ROESY (Rotating-frame Overhauser Enhancement SpectroscopY) spectra were collected with mixing times of 150 and 300 ms. A minimum of 2048 points were collected in t_2 with at least 256 points in t_1 and 32−64 scans per increment. 2D [$^1H-^1H$] DQF-COSY (Double-Quantum Filtered COrrelation SpectroscopY) spectra, collected with ^{31}P decoupling in both dimensions, resulted in a 1228 × 440 data matrix with 40 scans per increment. 2D [$^1H-^{31}P$] HETCOR (HETeronuclear shift CORrelation) spectra were collected with 2048 points in t_2, 112 points in t_1 with 512 scans per increment. The ^{31}P NMR spectral width was approximately 1500−3500 Hz. All data sets were processed using a 90° phase-shifted sine-bell apodization function and were zero-filled. The baselines were corrected with first or second order polynomials. Two-dimensional (2D) NMR data were processed using the program nmrPipe.[30]

The pH values of the samples were recorded on a Corning pH meter 430 equipped with a MI412 microelectrode probe by Microelectrodes, Inc. The pH dependences of the chemical shifts of several purine nuclei (^1H, ^{13}C, ^{31}P) were monitored by adding trace amounts of DCl and NaOD solutions. No correction was applied to the pH values for deuterium isotope effects on the glass electrode. pH titration curves were fitted to the Henderson−Hasselbalch equation using the program KALEIDAGRAPH,[31] with the assumption that the observed chemical shifts are weighted averages according to the populations of the protonated and deprotonated species.

MALDI (Matrix-Assisted Laser Desorption Ionization) mass spectra were acquired with an Applied Biosystems Voyager Elite XL mass spectrometer.

Molecular Modeling. Molecular modeling results were obtained using the software package Cerius^2 4.6 (Accelrys Inc., San Diego). To sample the conformational space of each compound, simulated annealing calculations in the gas phase were performed using the Open Force Field (OFF) program, with a modified version of the Universal Force Field (UFF).[32] The simulated annealing calculations were carried out for 80.0 ps, over a temperature range of 300−500 K, with $\Delta T = 50$ K, using the Nosé temperature thermostat, a relaxation time of 0.05 ps and a time step of 0.001 ps. The compounds were minimized (quenched) after each annealing cycle, producing 200 minimized structures. UFF is parametrized for octahedral Rh(III), whereas the molecules in the present study are metal−metal bonded Rh(II) compounds in a paddle-wheel structure with axial (*ax*) ligands. To account for the differences in the oxidation state and the coordination environment of the metal, the valence bond parameter was modified. The crystal structures of the HH $[Rh_2(OAc)_2(9\text{-EtGH})_2]^{2+}$ and HT $Rh_2(OAc)_2(9\text{-EtG})_2$ adducts[22a,b] were used to develop the appropriate valence bond parameter for these types of complexes. The original valence bond value of 1.3320 Å for Rh(III) was set to 1.2550 Å and all other parameters were left unmodified. The bond order for all bonds, except those including the Rh atoms, were calculated using the OFF bond order settings. The Rh−Rh and Rh−ligand bond orders were set to 1.0 and 0.5, respectively. The calculated Rh−Rh bond distances obtained for the lowest energy conformers of the HH and HT $Rh_2(OAc)_2(9\text{-EtG})_2$ isomers are 2.51 and 2.50 Å, respectively. The Rh−Rh, Rh−O and Rh−N bond distances are within 0.02, 0.05, and 0.1 Å of the crystal structure values, respectively, for both isomers.[22a,b] The energy difference between the minimized HH and HT isomers of $Rh_2(OAc)_2(9\text{-EtG})_2$ is less than 0.1 kcal/mol, consistent with the 1:1 ratio obtained from ^1H NMR spectroscopy (Table S2).[22a]

Results

I. 1D ^1H NMR Spectroscopy. a. $Rh_2(OAc)_2(9\text{-EtG})_2$. The aromatic region of the ^1H NMR spectrum of a lyophilized sample of $Rh_2(OAc)_2(9\text{-EtG})_2$ in D_2O, displays two resonances in 1:1 ratio.[22a] Due to the symmetry of the HH (C_{2v}) and HT (C_2) isomers (Chart 3), each set of H8 protons of bound 9-EtGH bases for each isomer gives rise to one resonance. Similarly, each of the two upfield resonances at $\delta = 1.92$ and 1.96 ppm, in 1:1 ratio, is ascribed to the set of equivalent bridging acetate groups for each isomer. The difference in solubility between the two isomers (the HT isomer is less soluble and therefore possible to remove from the reaction solution by fractional crystallization) allows for the assignment of the down- and upfield H8 resonances to the HH and HT isomers, respectively. The pH-dependent ^1H NMR titration curves of the H8 resonances for both isomers are depicted in Figure 1 (curves A, B). Protonation of the heterocyclic nitrogen atoms of guanine is known to have a strong influence on the ^1H NMR chemical shifts of the H8 proton.[4a] The pH-independent behavior of the H8 ^1H NMR resonances at low pH values (Figure 1, curves A and B) corroborates *N7* binding to rhodium for both isomers (the presence of the metal prevents protonation of this site); (de)protonation of *N7* and *N1* in unbound 9-EtGH take place at $pK_a \approx 2.5$ and 9.5, respectively (Figure 1, curve C).[25a] It is known that upon *N7* coordination to platinum, the pK_a value of *N1* decreases to ~8.5 due to an inductive effect of the metal.[4a,25c,33] For both $Rh_2(OAc)_2(9\text{-EtG})_2$ isomers, the substantial *increase* in the acidity of *N1*−*H* ($pK_a \approx 5.7$) (Figure 1, curves A and B) is attributed to *O6* binding to the dirhodium

(29) Markley, J. L.; Bax, A.; Arata, Y.; Hilbers, C. W.; Kaptein, R.; Sykes, B. D.; Wright, P. E.; Wüthrich, K. *Pure Appl. Chem.* **1998**, *70*, 117.
(30) Delaglio, F.; Grzesiek, S.; Vuister, G. W.; Zhu, G.; Pfeifer, J.; Bax, A. *J. Biomol. NMR* **1995**, *6*, 277.
(31) KALEIDAGRAPH, version 3.0.9; Synergy Software: Reading, PA, 1997.
(32) (a) Rappé, A. K.; Casewit, C. J.; Colwell, K. S.; Goddard III, W. A.; Skiff, W. M. *J. Am. Chem. Soc.* **1992**, *114*, 10024. (b) Castonguay, L. A.; Rappé, A. K. *J. Am. Chem. Soc.* **1992**, *114*, 5832. (c) Rappé, A. K.; Colwell, K. S.; Casewit, C. J. *Inorg. Chem.* **1993**, *32*, 3438.
(33) (a) Chu, G. Y. H.; Mansy, S.; Duncan, R. E.; Tobias, R. S. *J. Am. Chem. Soc.* **1978**, *100*, 593. (b) Marcelis, A. T. M.; Reedijk, J. *Recl. J. R. Neth. Chem. Soc.* **1983**, *102*, 121. (c) van der Veer, J. L.; van der Marel, G. A.; van den Elst, H.; Reedijk, J. *Inorg. Chem.* **1987**, *26*, 2272.

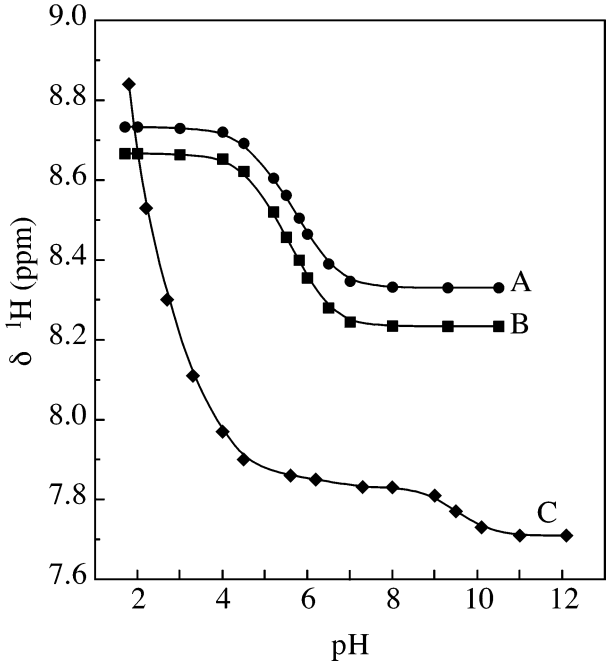

Figure 1. pH dependence of the H8 ^{1}H NMR resonances for (A) HH $Rh_2(OAc)_2(9\text{-EtG})_2$ (●), (B) HT $Rh_2(OAc)_2(9\text{-EtG})_2$ (■), and (C) unbound 9-EtGH (◆) in D_2O at 20 °C.

unit, a fact confirmed by the crystal structure of the HT isomer of $Rh_2(OAc)_2(9\text{-EtG})_2$ wherein 9-EtG$^-$ is deprotonated at *N1* (Chart 4b).[22a] It is thus inferred that *N1* experiences the effect of the bidentate *N7*/*O6* coordination to the metal accompanied by a *decrease* of its pK_a value by ∼2.5 log units as compared to the pK_a value, if *only N7* were bound to the metal. Facilitation of *N1*−*H* deprotonation upon metal interaction with *O6* of purines has been reported in the past.[34]

b. $Rh_2(OAc)_2${d(GpG)}. The aromatic region of the ^{1}H NMR spectrum of the dirhodium adduct in D_2O at pH 5.5, displays

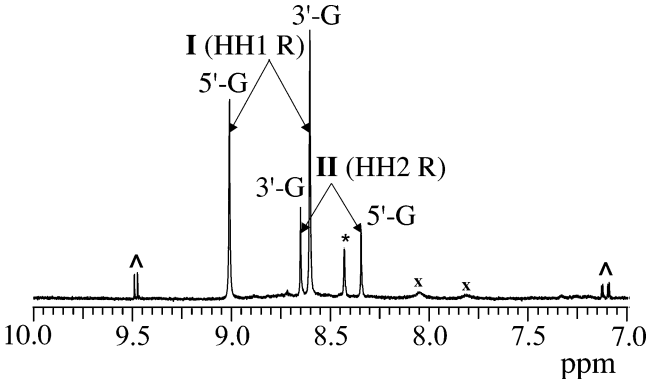

Figure 2. Aromatic region of the 1D ^{1}H NMR spectrum of the reaction products of $Rh_2(OAc)_4$ with d(GpG) in D_2O at 20 °C, pH 5.5, displaying the resonances of the H8 protons. The two dominant $Rh_2(OAc)_2$-{d(GpG)} adducts are **I** (HH1 R) and **II** (HH2 R); **x** indicates slight excess of d(GpG) and ∧ the presence of other minor products which are not characterized due to their limited quantities {a small D_2O impurity indicated with an asterisk (*) has been previously encountered in similar systems}.[16c]

(34) (a) Marzilli, L. G. In *Advances in Inorganic Biochemistry Vol. 3*; *Metal Ions in Genetic Information Transfer*; Eichhorn, G. L.; Marzilli, L. G., Eds.; Elsevier: North-Holland, New York, 1981; pp 47−82. (b) Marzilli, L. G.; de Castro, B.; Solorzano, C. *J. Am. Chem. Soc.* **1982**, *104*, 461 and references therein. (c) Abbott, D. W.; Woods, C. *Inorg. Chem.* **1983**, *22*, 1918.

Chart 5. Structure and Atom Numbering of $Rh_2(OAc)_2${d(GpG)}[a]

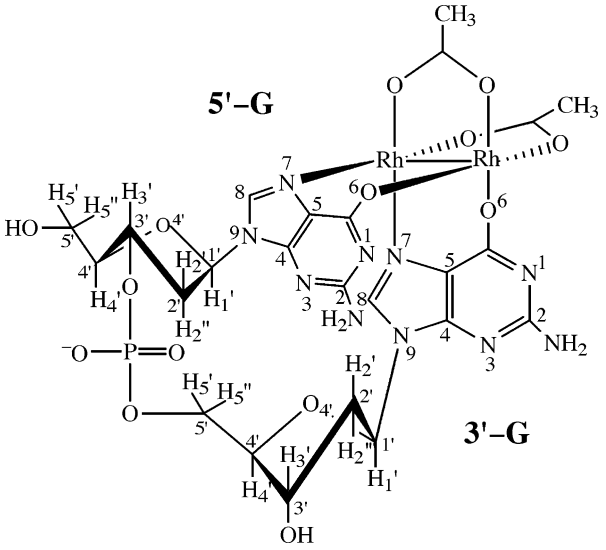

[a] Bond distances are not to scale and angles between atoms are distorted to show structure clearly.

two sets of nonequivalent H8 resonances, downfield from those of unbound d(GpG) (Figure 2), corresponding to two different isomers (**I** and **II**) *(vide infra)*. The pair of H8 resonances at δ = 9.01 and 8.60 ppm, attributed to isomer **I** (HH1 major isomer) is in an ∼3:1 ratio relative to the pair of H8 resonances at δ = 8.65 and 8.34 ppm, attributed to isomer **II** (HH2 minor isomer). The fact that these resonances are downfield from the H8 resonances of unbound d(GpG) at the same pH (δ = 8.05 and 7.81 ppm), and their pH independence at pH values near 2 (isomer **I**-Figure 3; isomer **II**-curves similar to those of isomer **I**) suggest guanine *N7* binding to the rhodium centers for both adducts (Chart 5).[4a,33,35] The assignment of the down- and upfield resonances at δ = 9.01 and 8.60 ppm to the 5′-G and 3′-G H8 protons of isomer **I** *(vide infra)*, respectively, was

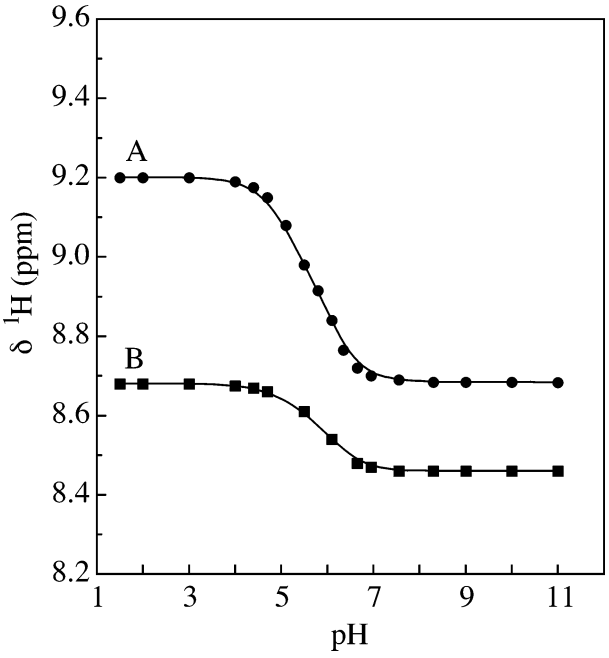

Figure 3. pH dependence of the two H8 ^{1}H NMR resonances for $Rh_2(OAc)_2${d(GpG)} major adduct **I** (HH1) in D_2O at 20 °C (A) 5′-G H8 (●), and (B) 3′-G H8 (■).

Table 1. ^{1}H and ^{31}P NMR Chemical Shifts (δ, ppm) for $Rh_2(OAc)_2${d(GpG)} and d(GpG)

d(GpG) species	G	H8	H1′	$^3J_{H1'-H2'}$/ $^3J_{H1'-H2''}$[a]	H2′	H2″	H3′	H4′	H5′/H5″	base sugar	^{31}P[b]
$Rh_2(OAc)_2${d(GpG)} HH1 R[c]	5′	8.80	6.23	0/7.3(d)	2.38	2.67	4.90	4.11	4.00[d]	*anti*	−3.38
	3′	8.58	6.24	10.6/5.1(dd)	2.83	2.44	4.66	4.17	3.93/4.07[e]	*anti*	
$Rh_2(OAc)_2${d(GpG)} HH2 R[c]	5′	8.23	6.19	0/6.6(d)	3.31	2.78	4.78	3.94	*f*	*anti*	−2.71
	3′	8.57	6.14	9.5/5.1(dd)	2.24	2.77	4.63	4.48	4.17/4.28[e]	*anti*	
d(GpG)[c]	5′	7.71	5.96		2.36	2.16	4.74	4.17	3.68[d]	*anti*	−4.00
	3′	8.00	6.08		2.77	2.47	4.77	4.18	4.09[d]	*anti*	

[a] In Hertz. [b] Relative to TMP (0 ppm). [c] pH 6.7, 5 °C. [d] Overlapped resonances. [e] Not stereospecifically assigned. [f] Not assigned due to resonance overlap.

accomplished by analysis of 2D NMR spectroscopic data. For the major adduct **I**, the two upfield resonances at $\delta = 1.98$ and 1.93 ppm, in 1:1 ratio, imply the presence of two nonequivalent bridging acetate groups bound to the dirhodium core (Chart 5). The down- and upfield resonances in the aromatic region at $\delta = 8.65$ and 8.34 ppm, attributed to the other set of H8 protons, are assigned to the 3′-G H8 and 5′-G H8 of the minor isomer **II**, respectively. The structures of both isomers are described in detail in the following section.

In Figure 3, the effect of *N1*−*H* deprotonation on the ^{1}H NMR chemical shifts of 5′-G H8 and 3′-G H8 is visualized {p$K_a \approx 5.7$ and 5.8 for curves A and B, respectively; p$K_a \approx$ 10.0 for unbound d(GpG)}; the substantially lowered pK_a values for $Rh_2(OAc)_2${d(GpG)} are comparable to those of the 9-EtGH adducts (Figure 1), and thus indicative of *O6* binding to the metal (in addition to *N7*). For *cis*-[Pt(NH$_3$)$_2${d(GpG)}][4a] and *cis*-[Pt(NH$_3$)(C$_6$H$_{11}$NH$_2$){d(GpG)}],[35] the pK_a value for *N1* (de)-protonation has been reported near 8.5, which is the expected value for *exclusive N7* binding to the metal. The effect of *N1* (de)protonation is more pronounced on 5′-G H8 than 3′-G H8, and the shapes of the H8 pH-dependent ^{1}H NMR titration curves are identical to those observed for the aforementioned platinum compounds except for the values of the inflection points. The shapes of the H8 pH-dependent ^{1}H NMR titration curves and the pK_a values of *N1* (de)protonation for the minor isomer **II** are very similar to those for the major isomer **I**, implying bidentate *N7/O6* binding of the purines in isomer **II** as well (Chart 5).

II. ^{13}C NMR Spectroscopy. For the aforementioned compounds, guanine binding to the dirhodium core via *O6* was corroborated by means of ^{13}C NMR spectroscopy. In Table S1 (Supporting Information), the values of the ^{13}C NMR chemical shifts for 9-EtGH, d(GpG) and their dirhodium bis-acetate adducts, at different pH values, have been summarized. At pH 7.0, *N1* of $Rh_2(OAc)_2(9\text{-EtG})_2$ is deprotonated (p$K_a \approx 5.7$, Figure 1) (*vide supra)* and the C6 ^{13}C NMR resonance for each $Rh_2(OAc)_2(9\text{-EtG})_2$ isomer exhibits a notable *downfield* shift of $\Delta\delta \approx 11.0$ ppm, whereas for C2 the shift is $\Delta\delta \approx 6.0$ ppm with respect to unbound 9-EtGH. If the comparison between the ^{13}C NMR chemical shifts of the $Rh_2(OAc)_2(9\text{-EtG})_2$ isomers and the unbound ligand is made at pH 4.0, then *N1* is protonated (Figure 1) and the downfield shifts for C6 and C4 are $\Delta\delta \approx$ 4.0 and 2.0 ppm, respectively, whereas C2 remains nearly unaffected. The substantial downfield effects on the ^{13}C NMR chemical shifts of C6, C2, and C4 (at the relevant pH) are afforded by *O6* binding to the rhodium centers and the ensuing enhancement in the acidity of *N1*−*H* (p$K_a \approx 5.7$).[34] In reported cases of exclusive *N7* binding of guanine and inosine nucleos-(t)ides to cisplatin, the resonances of C6 and C4 are upfield

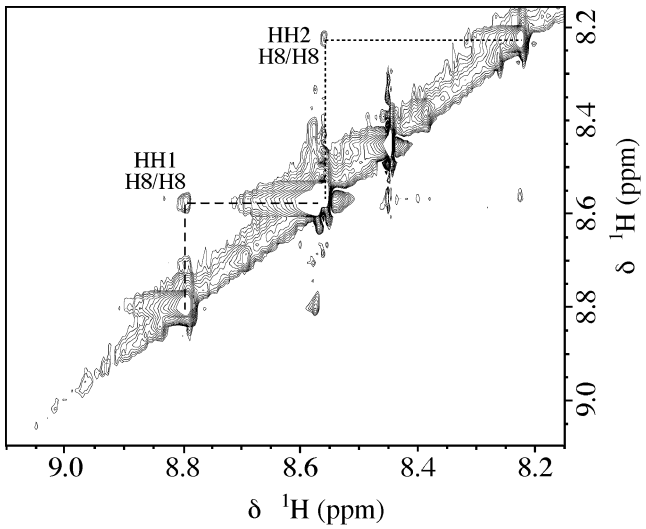

Figure 4. H8/H8 region of the 2D ROESY spectrum for conformers **I** (HH1) and **II** (HH2) of $Rh_2(OAc)_2${d(GpG)} in D$_2$O at 5 °C, pH 6.7. Intraresidue cross-peaks for HH1 are indicated with a medium dash (- - -) and those for HH2 with a dotted line (.....).

shifted by ∼1−3 and ∼1.5 ppm, respectively, whereas those of C2 are downfield shifted by ∼1−2 ppm.[34b,36,37] On the other hand, binding of guanosine or inosine to Rh(I) via *O6*, in the presence of a strong base, induces downfield shifts of ∼6 and 3 ppm for the guanosine C6 and C2 resonances, and ∼7 and 6 ppm for the inosine C6 and C2 resonances, respectively.[34b,c] It is therefore obvious that the $\Delta\delta \approx 11.0$ and 6.0 ppm *downfield* shifts, experienced by the C6 and C2 resonances of $Rh_2(OAc)_2(9\text{-EtG})_2$, are attributable to the additive effects of *O6* binding and *N1* deprotonation, facts that have been well established by the crystal structure of the HT isomer.[22a] The trend is also followed by the $Rh_2(OAc)_2${d(GpG)} adduct; namely at pH 8.0, the resonances of C6 and C2 are downfield shifted by $\Delta\delta \approx$ 11.0 and 6.0 ppm, respectively, with respect to unbound d(GpG) (Table S1); the latter supports *O6* binding in the aforementioned compound. The impact of the purine bidentate *N7/O6* binding to the dirhodium core is effectively visualized by plotting the ^{13}C NMR chemical shifts of C6 and C2 for 9-EtGH, and its dirhodium bis-acetate adducts as a function of pH (Figure S1). The pK_a of *N1* (de)protonation, derived from the pH-dependent ^{13}C NMR titrations for the $Rh_2(OAc)_2(9\text{-EtG})_2$ adducts, is estimated at ∼5.7, a value substantially lower than that of unbound 9-EtGH (p$K_a \approx 9.5$). As opposed to the dinucleotide adduct $Rh_2(OAc)_2${d(pGpG)}, for which ^{13}C NMR data col-

(35) Hartwig, J. F.; Lippard, S. J. *J. Am. Chem. Soc.* **1992**, *114*, 5646.

(36) Polissiou, M.; Viet, M. T. P.; St-Jacques, M.; Theophanides, T. *Inorg. Chim. Acta* **1985**, *107*, 203.

(37) (a) Buncel, E.; Norris, A. R.; Racz, W. J.; Taylor, S. E. *Inorg. Chem.* **1981**, *20*, 98. (b) Barbarella, G.; Bertoluzza, A.; Morelli, M. A.; Tosi, M. R.; Tugnoli, V. *Gazz. Chim. Ital.* **1988**, *118*, 637.

lection is possible at all pH values,[27] precipitation of the d(GpG) adduct at pH < 6.5 hampers detailed ^{13}C NMR data collection at these pH values and thus the relevant plot.

III. 2D NMR Spectroscopy. 2D ROESY, [^{1}H−^{1}H] DQF-COSY, and [^{1}H−^{31}P] HETCOR NMR spectra were collected to assign the H8 and sugar proton resonances of the $Rh_2(OAc)_2${d(GpG)} isomers (Table 1).

$Rh_2(OAc)_2${d(GpG)}. In the preceding 1D NMR section (Figure 2), two sets of downfield resonances, assigned to the major **I** (74%) and minor **II** (24%) isomers, have been discussed. Both isomers are present from the early stages of the reaction, although isomer **I** is thermodynamically more stable (after ∼18 days at room temperature, slow conversion of **II** to **I** takes place). The H8 resonances of a particular isomer are well separated and exhibit relatively intense H8/H8 ROE (Rotating frame nuclear Overhauser Effect) cross-peaks in the 2D ROESY NMR spectrum (Figure 4). These observations strongly support HH base orientation for both isomers (Chart 5).[13,16,27] *Head-to-tail* (HT) conformers lack this cross-peak because they have long H8−H8 distances; for comparison, the H8−H8 distances estimated for the HH $Rh_2(OAc)_2${d(GpG)} molecular models are in the range ∼2.9−3.2 Å for isomers **I** and **II**, and 6.5−6.8 Å for the HT isomers (*vide infra*, Table S3*)*. Three other sets of H8 resonances in the aromatic region are attributed to other minor products (Figure 2), but their low quantities prevented further studies (they are observed by ^{1}H NMR after ∼12 days of reaction at 37 °C). Due to this limitation, only the two abundant HH isomers have been further assigned.

The two sets of H8 ^{1}H NMR resonances, for the dominant $Rh_2(OAc)_2${d(GpG)} isomers, are assigned to the 5′-G and 3′-G residues by the following assessment: for the major HH isomer **I**, the downfield H8 resonance exhibits an H8/H3′ cross-peak in the 2D ROESY spectrum and this H3′ has a cross-peak to the phosphodiester ^{31}P NMR resonance in the [^{1}H−^{31}P] HETCOR spectrum, leading to an unequivocal assignment of the downfield H8 resonance to 5′-G, whereas H5′/H5″−^{31}P and H4′−^{31}P cross-peaks are observed for the 3′-G only (Figure 5, panel B);[13a,16] moreover, for the 3′-G sugar, H4′/H5′/H5″ and H5′/H5″ cross-peaks are observed in the [^{1}H−^{1}H] DQF-COSY spectrum (Figure 5, panel A). For the minor HH isomer **II**, the assignment is reversed with 3′-G and 5′-G H8 protons being down- and upfield, respectively.[16b,d] For both residues of isomer **I**, H8/H1′ ROE cross-peaks are absent, whereas 3′-G gives rise to strong H8/H2′/H2″ ROE cross-peaks, observations consistent with *anti* glycosidic torsion angles (Chart 5). Moreover, the 5′-G subunit exhibits strong H8/H3′ ROE cross-peaks along with H1′−H2″ (no H1′−H2′) DQF-COSY cross-peaks and a doublet coupling pattern for its H1′ in the [^{1}H−^{1}H] DQF-COSY spectrum (Figure S2); these findings imply C3′-endo (N-type) sugar ring conformation.[4a,b,13a,16b,d,33c,38] For isomer **II**, 5′-G has strong H8/H2′/H2″ and H8/H3′ ROE cross-peaks along with a doublet coupling pattern of its H1′ in the [^{1}H−^{1}H] DQF-COSY NMR spectrum (Figure S2), suggesting an *anti* oriented sugar ring with C3′-endo glycosidic conformation. Interestingly, for 3′-G of isomer **II** there are no observable H8/sugar cross-peaks in the 2D ROESY NMR spectrum (except for a very weak H8/H1′; this cross-peak along with the quartet at 6.14 ppm in the 1D ^{1}H NMR spectrum led to its assignment). Both the absence of H8/H3′ ROE cross-peaks, and the doublet of doublets coupling pattern observed in the [^{1}H−^{1}H] DQF-COSY NMR spectrum (Figure S2), easily discerned from the 1D ^{1}H NMR spectrum as well, for the 3′-G H1′ residues of both isomers, are indicative of 3′-G S-type sugar ring conformation.[16,38]

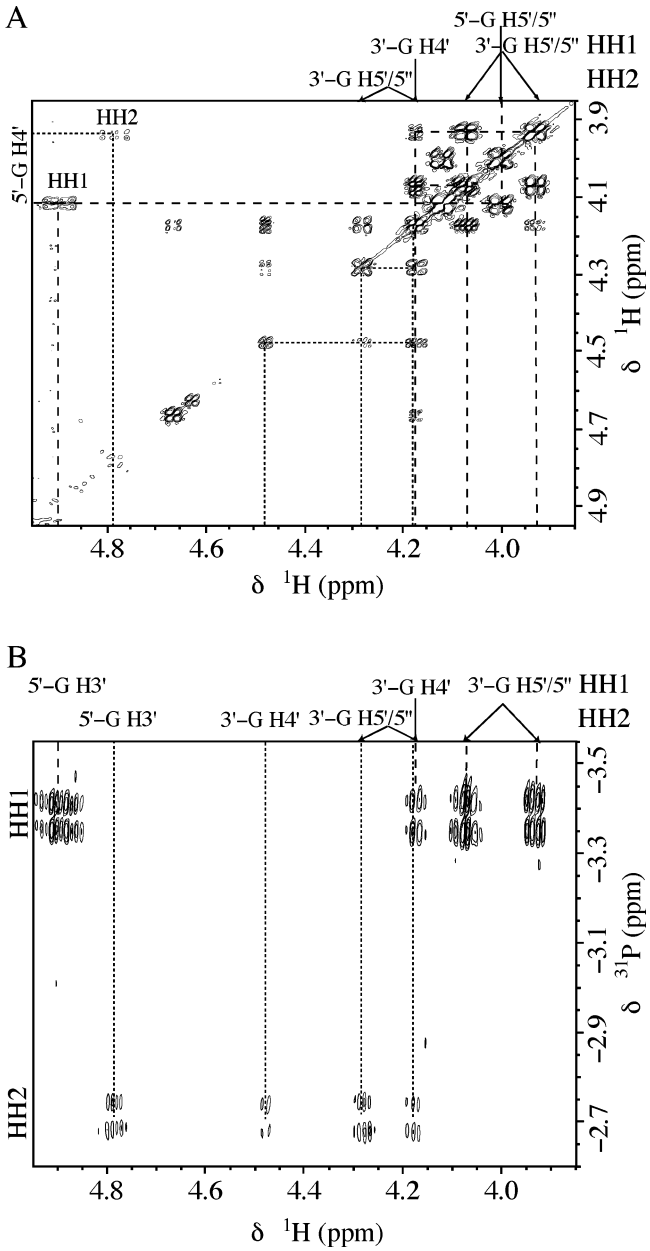

Figure 5. Related regions of the 2D [^{1}H−^{1}H] DQF-COSY and [^{1}H−^{31}P] HETCOR spectra for conformers HH1 and HH2 of $Rh_2(OAc)_2${d(GpG)} in D_2O at 5 °C, pH 6.7 (A) H3′/H4′/ H5′/ H5″ region of the [^{1}H−^{1}H] DQF-COSY spectrum, and (B) region of the [^{1}H−^{31}P] HETCOR spectrum for the phosphate diester groups {δ (^{31}P) = − 3.38 and − 2.71 ppm for HH1 and HH2, respectively}; cross-peaks for HH1 are indicated with a medium dash (- - -) and those for HH2 with a dotted line (.....). The sugar protons are labeled at the top of the spectra; all protons labeled on the same level with HH1 and HH2 belong to the relevant conformer. The traces of the sugar protons that couple to ^{31}P nuclei ([^{1}H−^{31}P] HETCOR spectrum, panel B) are followed to the [^{1}H−^{1}H] DQF-COSY spectrum (panel A) with dotted (or dashed) lines.

The aforementioned conformational features of the two HH $Rh_2(OAc)_2${d(GpG)} isomers (*anti* oriented sugars with S- and N-type conformations for the 3′-G and 5′-G residues, respectively) imply a great degree of similarity between them with

(38) Widmer, H.; Wüthrich, K. *J. Magn. Reson.* **1987**, *74*, 316.

Chart 6. Illustration of the Possible Head-to-Head (HH) Variants of $Rh_2(OAc)_2\{d(GpG)\}$ with (A) Left (L) Canting[a] (B) Right (R) Canting and (C) Stick Models of HH R Variants

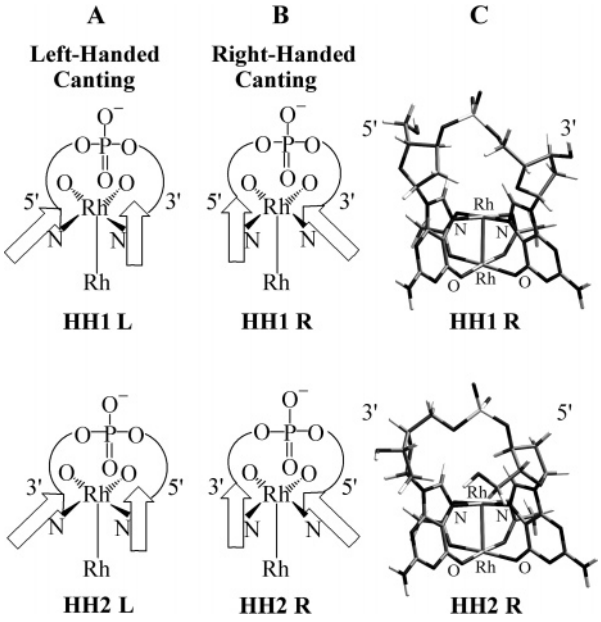

[a] Canting arises from the fact that the G bases are not oriented exactly perpendicular to the N7−Rh−N7 plane. (A) Left-handed models of $Rh_2(OAc)_2\{d(GpG)\}$. (B) Right-handed models of $Rh_2(OAc)_2\{d(GpG)\}$; 1 and 2 refer to models with 5′-G and 3′-G positioned to the left, respectively. In parts A and B, viable comparisons with the Pt models are made by considering the two rhodium atoms as face-to-face square planes with the Rh atom attached to the N7 atoms depicted on the top and the oxygen atoms of the attached acetate groups in the back; to show the structures clearly, the coordination sites for the second Rh atom are not shown, thus the O6 binding of G is not depicted. The G base is indicated with an arrow having H8 at the tip. (C) Representative stick models of the HH1 R (upper panel) and HH2 R (lower panel) $Rh_2(OAc)_2\{d(GpG)\}$ conformers identified in solution.

one important exception, namely isomers **I** and **II** exhibit upfield 3′-G and 5′-G H8 resonances, respectively. The reversed order of the H8 resonances for the two HH isomers may be accounted for by invoking a difference in the direction of propagation of the phosphodiester backbone with respect to 5′-G, an insightful interpretation refined by Marzilli *et al.*,[16] initially proposed by Kozelka *et al.*[5c,d] By adopting the schematic representations and nomenclature generally accepted for the *cis*-$[PtA_2\{d(GpG)\}]$ conformers, the possible variants for the dirhodium isomers have been sketched (Chart 6; panels A and B). The HH1 L and HH2 R variants have the same relative canting of the bases but differ in the direction of propagation of the phosphodiester backbone with respect to 5′-G. It is well documented from cisplatin and its derivatives that HH cross-links usually have one base canted toward the other and the H8 of the more canted base is shifted upfield due to the ring current effects of the less canted base, *i.e.*, the H8 chemical shift relationship depends on the relative canting.[16]

For the $Rh_2(OAc)_2\{d(GpG)\}$ isomers, **I** gives rise to an upfield 3′-G H8 resonance and can therefore be identified as the HH1 R or HH2 L variant. By applying the same reasoning to isomer **II**, which has an upfield 5′-G H8 resonance, it is inferred that it is either the HH1 L or HH2 R variant. Subtle differences of the two isomers in the 2D NMR spectra,[39] comparison with reported platinum compounds with similar features[16a−c,40] accompanied by the molecular modeling results presented in the following section, have led to the conclusion that isomers **I** and **II** are HH1 and HH2 variants, respectively; therefore, isomer **I** is associated with HH1 R (Chart 6C, upper panel) and isomer **II** with HH2 R (Chart 6C, lower panel).

IV. ^{31}P NMR Spectroscopy. $Rh_2(OAc)_2\{d(GpG)\}$. The 1D ^{31}P NMR spectrum displays two resonances at $\delta = -3.38$ and -2.71 ppm (Table 1), assigned to the major **I** (HH1 R) and minor **II** (HH2 R) isomers, respectively, based on the intensity ratio. Both resonances are downfield from that of the unbound dinucleotide d(GpG) ($\delta = -4.00$ ppm), and the resonance of the HH2 R isomer is further downfield from that of HH1 R; the same chemical shift ordering relationship was observed for the *(R,S,S,R)*-BipPt{d(GpG)} isomers,[16a−c] a finding which supports the previous isomer assignment to HH1 R and HH2 R. Typically, for HH isomers, the H8 protons and the phosphate groups resonate downfield from the unbound dinucleotide.[4a,b,12,13a,16b,33c,41] Downfield shifting of the ^{31}P NMR resonances in DNA usually indicates an increase in the unwinding angle characterized by changes in the R−O−P−OR′ torsion angles.[13a,42] The downfield ^{31}P NMR chemical shifts observed for d(GpG) containing oligonucleotide adducts with platinum and other metals imply that, when adjacent guanine residues bind to the metal, an extension of the conformation about the diester bond between the G bases occurs.[43]

V. Molecular Modeling. Models of the dirhodium adducts were constructed and subjected to simulated annealing calculations. Energy differences of a few kcal/mol were treated cautiously and have been interpreted in conjunction with the spectroscopic data. Conformational features determined by NMR spectroscopy were reproduced well by the calculations.

The HH and HT models constructed for $Rh_2(OAc)_2(9\text{-EtG})_2$ were deprotonated at *N1*, despite the fact that the available HH structure is protonated,[22b] to allow for a meaningful comparison of the relative energies for the two species. The two isomers are nearly isoenergetic, (within 0.1 kcal/mol-all the lowest energy HH and HT models are within 0.3 and 0.4 kcal/mol, respectively; Table S2), a result that supports their presence in 1:1 ratio in solution (as inferred from ^{1}H NMR spectroscopic data).

In the case of tethered adducts, the HH1 and HH2 variants of $Rh_2(OAc)_2\{d(GpG)\}$ were considered. For both directions, the lowest energy models are *right-handed* (Chart 6C) with HH1 being 1 kcal more stable than HH2. These findings support the existence of two right-handed adducts in solution (HH1 R and HH2 R variants; *vide supra*), with conformer HH1 R (74%) (Figure 6A) three times more abundant than HH2 R (24%) (Figure 6B) (Table S3). The possible left-handed models for both HH1 and HH2 variants (Chart 6A) are higher in energy.

(39) There are no observable H8/sugar ROE cross-peaks for 3′-G of isomer HH2 R, whereas for 3′-G of isomer HH1 R such peaks are present; for 5′-G of isomer HH1 R, only a strong H8/H3′ ROE is present, whereas for isomer HH2 R there are strong 5′-G H8/H3′ and H8/H2′ ROE cross-peaks, an indication that there are slight differences in the orientations of the 5′-G bases with respect to the glycosyl bonds.
(40) The $Rh_2(OAc)_2\{d(GpG)\}$ HH1 R and HH2 R conformers have the same relative order of the H8 resonances as those of the *(R,S,S,R)*-BipPt{d(GpG)} HH1 R and HH2 R isomers, respectively, and similar observations have been made for the corresponding isomers in the 2D NMR spectra; Bip = 2,2′-bipiperidine.[16a−c]
(41) Bloemink, M. J.; Heetebrij, R. J.; Inagaki, K.; Kidani, Y.; Reedijk, J. *Inorg. Chem.* **1992**, *31*, 4656.
(42) Gorenstein, D. G. *In Phosphorus-31 NMR.; Gorenstein*, D. G., Ed.; Academic: New York, 1984.
(43) Spellmeyer Fouts, C.; Marzilli, L. G.; Byrd, R. A.; Summers, M. F.; Zon, G.; Shinozuka, K. *Inorg. Chem.* **1988**, *27*, 366.

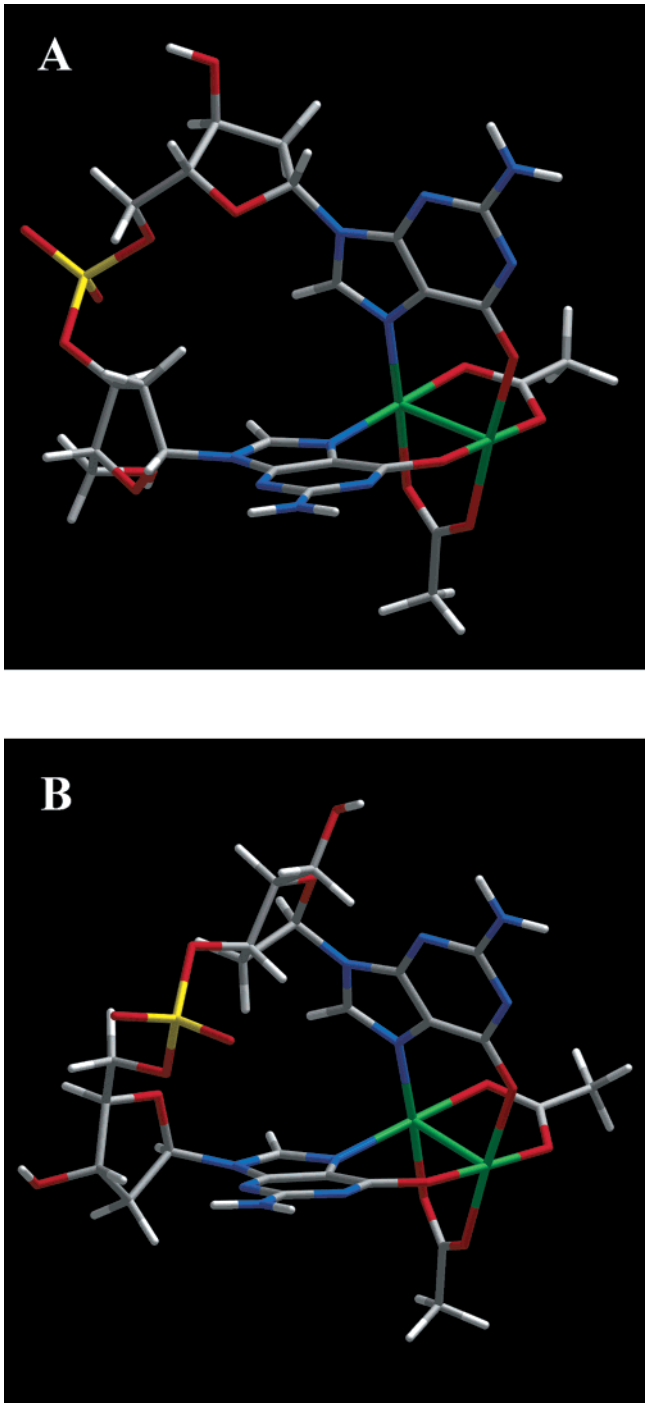

Figure 6. Lowest energy conformers, resulting from simulated annealing calculations, for the experimentally observed right-handed variants of $Rh_2(OAc)_2${d(GpG)} (A) HH1 R and (B) HH2 R. Color code: Rh green, N blue, O red, P yellow, C gray, H white.

The measured interproton distances are in agreement with the relative intensities of the ROE cross-peaks,[39] *i.e.*, the distances from the H8 to the sugar ring protons H3′/H2′/H2″ for 3′-G of HH2 R are > 4.5 Å, and thus preclude the appearance of ROE cross-peaks. On the contrary, for the 3′-G of HH1 R, the distance H8/H2′ ∼ 2.6 Å supports the appearance of an H8/H2′ ROE cross-peak, whereas the 5′-G N- and 3′-G S-type sugar conformations are verified for both HH R conformers. For both HH isomers, the H8−H8 distances are in the range ∼2.9−3.2 Å (Table S3), thus corroborating relatively intense H8/H8 cross-peaks in the 2D ROESY NMR spectrum (Figure 4; *vide supra*). It is noteworthy that the $Rh_2(OAc)_2$-{d(GpG)} models considered have the two guanine bases binding in a bridging fashion via *N7/O6* (Chart 5). Models built with each guanine chelating to one Rh(II) center via *N7/O6* are 44 kcal higher in energy than the bridging models; the chelating bases impose conformational strain on the phosphate backbone, a fact that effectively eliminates the need to consider such modes as viable.

Discussion

N7/O6 Binding of the Dirhodium Adducts. The two isomers of $Rh_2(OAc)_2(9\text{-EtG})_2$ have been used as models to gain insight into the binding mode of d(GpG) to the antitumor active compound $Rh_2(OAc)_4$. The X-ray structural determinations of the dirhodium tetraacetate substitution products with 9-EtGH have unequivocally shown that guanine adopts unprecedented *eq N7/O6* bridging interactions,[22a,b] apart from *ax N7*-bound guanine derivatives observed for other dirhodium(II,II),[20i] and diplatinum(III,III)[44] compounds.

Contrary to the clear preference of HT conformers for mononuclear platinum adducts with untethered bases,[7−11] the $Rh_2(OAc)_4$ reaction proceeds with formation of the HH and HT isomers in 1:1 ratio.[22a] The presence of the two isomers in equal amounts (a finding reproduced by the simulated annealing calculations) is based on the 1:1 ratio of the two H8 ^{1}H NMR resonances. The two isomers were traced in solution by pH dependence studies of the H8 ^{1}H NMR resonances (Figure 1, curves A and B). As expected, no *N7* protonation is observed at pH < 3.0 for both adducts due to *N7* binding to the metal; furthermore, a substantial enhancement in the acidity of *N1−H* (the pK_a value has decreased to ∼5.7 as compared to ∼9.5 for unbound 9-EtGH[25a] and ∼8.5 for *N7 only* bound adducts[4a,33]) is exhibited by both isomers. The substantial *increase* in the acidity of *N1−H* implies *O6* binding to the dirhodium unit. There is precedent for facilitation of *N1−H* deprotonation upon metalation[34] or methylation[45] of *O6*, thus rendering the pK_a value of *N1−H* a valuable probe for detecting *O6* binding.

The pH-dependent ^{1}H NMR titration curves for the H8 resonances of the $Rh_2(OAc)_2${d(GpG)} isomers **I** (HH1) (Figure 3) and **II** (the curves for HH2 are similar to those in Figure 3) closely resemble those of $Rh_2(OAc)_2(9\text{-EtG})_2$ (Figure 1), *i.e.*, no *N7* protonation is observed at low pH and the pK_a values of *N1−H* deprotonation have decreased to ∼5.7 and ∼5.8 for 5′-G H8 and 3′-G H8, respectively, the latter effects induced by purine binding to the rhodium centers via *N7/O6*; in particular, *O6* binding to rhodium promotes facilitation of *N1−H* deprotonation. For comparison, exclusive *N7* binding in *cis*-[$Pt(NH_3)_2$-{d(GpG)}][4a,33] and *cis*-[$Pt(NH_3)(C_6H_{11}NH_2)${d(GpG)}][35] affords values pK_a ≈ 8.5 for *N1−H* (de)protonation.

The *enhanced* acidity of *N1−H*, reflecting the participation of guanine *O6* in rhodium binding, has been corroborated by the pH dependence studies of the C6 and C2 ^{13}C NMR resonances for $Rh_2(OAc)_2(9\text{-EtG})_2$ and 9-EtGH (Figure S1; poor solubility of $Rh_2(OAc)_2${d(GpG)} at pH < 6.5 precluded it from

(44) (a) Kampf, G.; Willermann, M.; Zangrando, E.; Randaccio, L.; Lippert, B. *Chem. Commun.* **2001**, 747. (b) Kampf, G.; Willermann, M.; Freisinger, E.; Lippert, B. *Inorg. Chim. Acta*, **2002**, *330*, 179 and references therein. (c) Ito, K.; Somazawa, R.; Matsunami, J.; Matsumoto, K. *Inorg. Chim. Acta*, **2002**, *339*, 292.
(45) Struik, A. F.; Zuiderwijk, C. T.; van Boom, J. H.; Elding, L. I.; Reedijk, J. *J. Inorg. Biochem.* **1991**, *44*, 249.

such a study). From these studies, it is obvious that the pK_a value of *N1−H* (de)protonation decreases from ∼9.5 for the unbound 9-EtGH to ∼5.7 for the dirhodium adducts. The pK_a values estimated for *N1−H* (de)protonation from the pH dependence studies of the ^{13}C NMR resonances concur with those derived from the H8 ^{1}H NMR resonance titrations and strongly reflect the effect of *O6* binding to the dirhodium centers. Moreover, *O6* binding is unambiguously evidenced by comparison of the ^{13}C NMR resonances of C6 and C2 for the dirhodium adducts $Rh_2(OAc)_2$(9-EtG)$_2$ and $Rh_2(OAc)_2${d(GpG)} with the corresponding resonances of the unbound ligands {at pH 7.0 for 9-EtGH and pH 8.0 for d(GpG); Table S1}; substantial downfield shifts of $\Delta\delta \approx 11.0$ and 6.0 ppm for C6 and C2, respectively, lend credence to the aforementioned argument about *O6* binding to the dirhodium core.

For the dirhodium adducts, the ^{13}C NMR resonances of C5 experience only small downfield shifts upon *O6* metal binding, as previously noted in the literature;[34b] this downfield impact on the ^{13}C NMR resonance of C5, upon *O6* binding, may be partially balanced by the expected ∼3 ppm upfield shift (observed in cisplatin adducts) due to *N7* binding to the metal.[34b,36,37] The ^{13}C NMR resonance of C8 usually experiences an ∼3 ppm downfield shift upon *N7* metal binding.[36,37] Although this behavior is followed by the 9-EtGH adducts with dirhodium bis-acetate (Table S1), the expected downfield shift of the C8 resonance is not observed for the tethered d(GpG) adduct; this deviation from the expected trend followed by the untethered bases, has also been encountered in single-stranded (*ss*) [d(TG*G*T)-N7/N7]-Pt(en)[46a] and double-stranded (*ds*) [d(CTCCG*G*CCT)-N7/N7]-Pt$(NH_3)_2$ complexes;[46b] for the former, this has been attributed to the "nonideal" overlap of the *N7* lone pairs of both guanine bases with the metal center due to metal induced distortion of the DNA structure, as well as to heavy-atom anisotropic effects of Pt on the ^{13}C NMR chemical shifts.

Conformational Characteristics of the $Rh_2(OAc)_2${d(GpG)} Adduct. Apart from the *N7/O6* primary binding sites, the nature and conformational characteristics of the $Rh_2(OAc)_2${d(GpG)} adduct have been assessed by 2D NMR spectroscopy. Upon tethering the two metalated guanine bases through the phosphodiester bond, the two dinucleotide H8 protons become nonequivalent. In addition to the deshielding effect of the metal on both rings, the more canted base experiences an upfield shifting effect due to the ring-current anisotropy of the other *cis* base.[5c,d] It is well documented from the studies of Pt compounds, that the guanine bases are not oriented exactly perpendicular to the coordination plane, and that the degree and direction of canting (Chart 6) depends on the carrier ligands (in the case of cisplatin, the amine groups), the presence of a linkage between the bases, the sugar (deoxyribose or ribose), the presence of a 5′-flanking residue and the *ss* or *ds* structure of the DNA.[5c,16d,17] The $Rh_2(OAc)_2${d(GpG)} adduct gives rise to two dominant isomers which have downfield and disparate H8 proton resonances and relatively intense H8/H8 ROE cross-peaks; these features are consistent with HH conformers.[4a,13,16,27] The opposite H8 chemical shift relationship of the two isomers (isomers **I** and **II** exhibit upfield 3′-G and 5′-G H8 resonances, respectively) implies a difference in the direction of propagation of the phosphodiester backbone with respect to 5′-G for the two isomers (Chart 6). In accordance with the recently assessed rules for base canting, the H8 resonance of the more canted base (and thus more shielded) moves upfield due to the ring current effects of the less canted base;[16a,b] therefore 3′-G is more canted in **I**, whereas 5′-G is more canted in **II**. The striking similarities in the ^{1}H, ^{31}P and 2D NMR spectra of the $Rh_2(OAc)_2${d(GpG)} isomers **I** and **II** with respect to the *(R,S,S,R)*-BipPt{d(GpG)} HH1 R and HH2 R conformers[16a−c,40] (accompanied by the simulated annealing results, which predict right-handed variants as the most stable) lead to the logical assignment of the two $Rh_2(OAc)_2${d(GpG)} conformers to the right-handed variants HH1 R and HH2 R (Chart 6C and Figure 6). The HH2 variants of platinated d(GpG) adducts have been elusive due to the degree of fluxionality in cisplatin and were first identified by Marzilli *et al.* by invoking retro models with carrier ligands on the platinum center that decrease the fluxional motion above and below the conformational plane.[16,17] In the case of $Rh_2(OAc)_2${d(GpG)}, it is logical to conclude that the unusual minor HH2 R conformer was observed in view of the combined effects of restricted rotation of the guanine about the N7−Rh bond due to *O6* binding, and the presence of the sterically encumbering acetate groups. Although HH2 conformers are unlikely to exist in a duplex at low temperature, they may be important in mutational events, duplex breathing, or duplex interactions with DNA recognition proteins and repair enzymes.[1e,16a,c] The major $Rh_2(OAc)_2${d(GpG)} HH1 isomer is also unusual in the sense that it is an R minihelix variant (with opposite chemical shift relationship of the 3′-G and 5′-G H8 protons as compared to *cis*-[Pt$(NH_3)_2${d(GpG)}], which has 3′-G H8 downfield from 5′-G H8), whereas HH1 L variants of *ss* d(GpG) platinum adducts appear to be dominant in solution,[5c,d] except for three other reported cases.[13b,16a,c,47] In duplexes with the *cis*-Pt$(NH_3)_2${d(GpG)} moiety, however, the HH1 R variants (with the 5′-G H8 downfield from 3′-G H8) appear to dominate.[5c,d] In this respect, $Rh_2(OAc)_2${d(GpG)} HH1 R is a better model than *cis*-[Pt$(NH_3)_2${d(GpG)}] for the duplex DNA cross-link lesion.[16]

The assessment of the 2D NMR spectral features for both HH1 R and HH2 R $Rh_2(OAc)_2${d(GpG)} variants (Chart 6C and Figure 6) revealed *anti* oriented sugars, retention of C2′-endo (S-type) and alteration to C3′-endo (N-type) deoxyribose conformations for the 3′-G and 5′-G units, respectively. These notable features bear close resemblance to those of *cis*-[Pt$(NH_3)_2${d(GpG)}], which is documented to exist as a HH cross-linked adduct with *anti* oriented 5′-G and 3′-G sugar rings in the C3′-endo and C2′-endo conformations, respectively.[4b] The similarities between the cisplatin and the dirhodium d(GpG) adducts can be further appreciated in the following paper of this issue wherein low energy conformers of $Rh_2(OAc)_2${d(pGpG)} are compared with the crystal structure of *cis*-[Pt$(NH_3)_2${d(pGpG)}].[27]

Conclusions

The results of the present study provide unambiguous structural evidence that GG containing DNA fragments bind *equatorially* to the dirhodium unit. The two octahedral rhodium atoms provide *cis* sites for covalent binding of the tethered guanine bases via *N7*/*O6* bridges spanning the Rh-Rh bond. The effects of the bidentate *N7/O6* binding of the guanine nucleo-

(46) (a) Mukundan, S.; Xu Y.; Zon, G.; Marzilli, L. G. *J. Am. Chem. Soc.* **1991**, *113*, 3021 and references therein. (b) Marzilli, L. G.; Saad, J. S.; Kuklenyik, Z.; Keating, K. A.; Xu Y. *J. Am. Chem. Soc.* **2001**, *123*, 2764.

(47) Dunham, S. U.; Lippard, S. J. *J. Am. Chem. Soc.* **1995**, *117*, 10 702.

bases, in addition to the presence of the bulky acetate groups on the dirhodium core, allowed for the identification of unusual HH right-handed conformers for *ss* DNA in solution. The present characterization of the HH1 R and HH2 R conformers for $Rh_2(OAc)_2$\{d(GpG)\} adds to the database of information about conformational diversity of *cis*-[$Pt(NH_3)_2$\{d(GpG)\}] adducts in solution, the latter being elusive due to the rotational freedom about the Pt−N7 bond. The conformational features of the metal-DNA formed lesions may have an impact on the activity of the drugs due to mutational events or duplex interactions with cellular proteins.

A notable point of this study relates to the *N7/O6* binding to the dirhodium core with the consequential large decrease of the pK_a value of *N1* by ∼2.5 log units as compared to 1 pK_a unit for exclusive *N7* binding to cisplatin, a fact which may lead to interesting biological implications. This *N7/O6* binding mode would interrupt the Watson−Crick hydrogen bonding to *O6*, and at a physiological pH, nearly all of the *N7/O6* lesions in the DNA chain would be deprotonated at *N1*, which is a site that also participates in interstrand hydrogen bonding. The implications of this behavior remain to be determined.

Efforts are in progress to characterize the adducts of longer oligonucleotides and duplexes with dirhodium carboxylate complexes and their derivatives.

Acknowledgment. Professor Jan Reedijk is gratefully acknowledged for insightful discussions and crucial suggestions. Dr. Steven K. Silber and Dr. Michael Angel provided valuable technical assistance with the ^{13}C NMR data collection. The authors thank the reviewers for helpful comments. The Laboratory for Molecular Simulation at Texas A&M University is acknowledged for providing software and computer time. Use of the TAMU/LBMS-Applications Laboratory (Laboratory of Biological Mass Spectroscopy) and Dr. John M. Koomen are also acknowledged. K.R.D. thanks Johnson-Matthey for a generous loan of dirhodium tetraacetate. The NMR instrumentation in the Chemistry Department at Texas A&M University was funded by NSF (CHE-0077917). The NMR instrumentation in the Biomolecular NMR Laborartory at Texas A&M University was supported by a grant from the National Science Foundation (DBI-9970232) and the Texas A&M University System. K.R.D. thanks the State of Texas for an ARP grant (010366-0277-1999), and the Welch Foundation (A1449) for financial support.

Supporting Information Available: Table with ^{13}C NMR chemical shifts for 9-EtGH, d(GpG) and their dirhodium bis-acetate adducts in D_2O; table with summary of energies from simulated annealing calculations and experimentally observed percent of dirhodium bis-acetate adducts; table with summary of energies, selected distances and angles for the $Rh_2(OAc)_2$-\{d(GpG)\} isomers; pH dependence of the ^{13}C NMR resonances for nuclei C6 and C2 of the $Rh_2(OAc)_2(9\text{-EtG})_2$ isomers and unbound 9-EtGH in D_2O at 20 °C; H1′ and H2′/H2″ regions of the [^1H-^1H] DQF-COSY NMR spectrum of the HH1 and HH2 $Rh_2(OAc)_2$\{d(GpG)\} conformers in D_2O at 5 °C, pH 6.7; MALDI mass spectrum for $Rh_2(OAc)_2$\{d(GpG)\}. This material is available free of charge via the Internet at http://pubs.acs.org.

JA027779S